

Early Stages of Homopolymer Collapse

A. Halperin

*UMR 5819 (CEA-CNRS-UJF), DRFMC,
CEA-Grenoble, 17 rue des Martyrs,
38054 Grenoble Cedex 9, France*

Paul M. Goldbart

*Department of Physics,
University of Illinois at Urbana-Champaign,
1110 West Green Street,
Urbana, Illinois 61801-3080, U.S.A.
(May 20, 1999)*

Abstract: Interest in the protein folding problem has motivated a wide range of theoretical and experimental studies of the kinetics of the collapse of flexible homopolymers. In this Paper a phenomenological model is proposed for the kinetics of the early stages of homopolymer collapse following a quench from temperatures above to below the θ temperature. In the first stage, nascent droplets of the dense phase are formed, with little effect on the configurations of the bridges that join them. The droplets then grow by accreting monomers from the bridges, thus causing the bridges to stretch. During these two stages the overall dimensions of the chain decrease only weakly. Further growth of the droplets is accomplished by the shortening of the bridges, which causes the shrinking of the overall dimensions of the chain. The characteristic times of the three stages respectively scale as N^0 , $N^{1/5}$ and $N^{6/5}$, where N is the degree of polymerization of the chain.

PACS: 61.25.Hq, 83.10.Nn

I. INTRODUCTION

The purpose of this Paper is to discuss the evolution of the structure of a single polymer molecule after the environment has been changed from a good solvent to a poor solvent. Our approach is via a phenomenological model for the kinetics of the early stages of collapse. We have in mind a long flexible polymer chain immersed in a simple solvent, and a change in the temperature T as the means of altering the solvent quality. The initial state is one of equilibrium in a good solvent, in which the chain is swollen and has radius of gyration $R = R_F \sim N^{3/5}$, where N is the degree of polymerization. The final state is one of equilibrium in a poor solvent, in which the chain is collapsed into a dense, spherical globule, i.e., $R = R_c \sim N^{1/3}$. The variation of the equilibrium state with the solvent quality is, with some important caveats, well understood [1–4]. In marked contrast, there is no comparable consensus concerning the kinetics of collapse following an abrupt T quench, i.e., a rapid change in temperature from above to below the θ temperature. The experimental picture is not clear because of difficulties due to the competition between the collapse of the individual chains and the aggregation of different ones. As a result, there have been only few experimental studies of the kinetics of collapse of isolated chains [5–7]. Theoretical studies have utilized a variety of approaches in focusing on different aspects of the problem. Langevin models [8–10], phenomenological models [11–13] and computer simulations [14–20] have been used to consider the kinetics of collapse in the absence of topological constraints. Other studies have focused on the role of internal entanglements [21,22] or the competition with chain-chain aggregation [23,24]. In spite of the extensive activity in this area, a complete picture of the kinetics of collapse has yet to emerge. The search for such picture is motivated primarily by the intense current interest in the protein folding question [25–27] because early stages of protein folding are thought to proceed as the collapse of flexible homopolymers.

The collapse of a flexible chain following an abrupt change of solvent quality displays certain features of a first-order phase transition. These features occur for chains of finite N for which the surface free energy of the globule plays an important role. Two such features are important to the present discussion. First, the onset of collapse involves, as we shall discuss, the formation of droplets of the dense “phase”. Second, the collapse proceeds via intermediate states corresponding to the “tadpole” configuration of a stretched, collapsed globule [28], which involve the coexistence of dense globules and strongly stretched segments. With this picture in mind, it is possible to distinguish between four stages in the kinetics of collapse (Fig. 1). Each stage is characterized by a length-scale and a time-scale. The characteristic time scale increases with the relevant length scale. The formation of p ($\ll N$) droplets of the dense

phase, which we refer to as “pearls”, is the fastest process. This “pearling” stage involves local rearrangement of the chain configurations within the randomly placed droplets during which the dimensions and configurations of the chain as a whole are only weakly modified. The

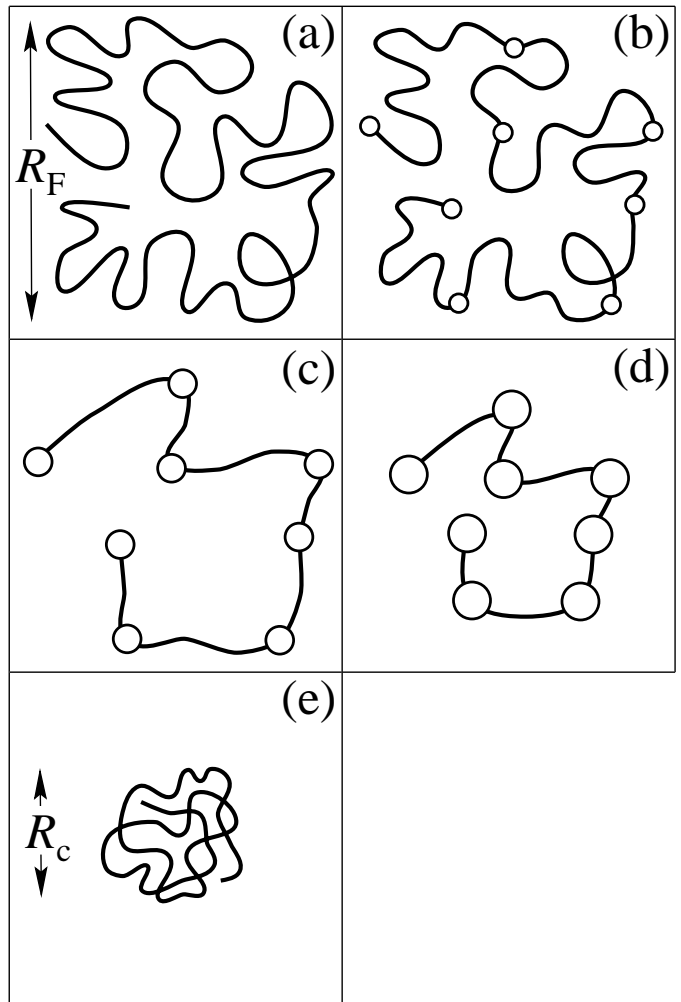


FIG. 1. Proposed sequence of states during the collapse of a flexible homopolymer:
(a) self-avoiding configuration under good solvent conditions;
(b) pearling;
(c) bridge stretching;
(d) collapse of the pearl necklace;
(e) equilibrium collapsed configuration in a poor solvent.

nascent droplets then grow by accreting monomers from the bridges that connect them. The positions of the growing droplets are roughly stationary and their growth is accommodated by the gradual stretching of the bridges. This “bridge-stretching” stage ends when the tension in the bridges attains the equilibrium value f_{co} corresponding to the “tadpole” configuration of a stretched globule. During this process the dimensions of the chain as a whole remain essentially constant i.e., $R \sim N^{3/5}$, but the configurations of the bridges are qualitatively mod-

ified. The number of droplets p is set by the requirement that $R \sim N^{3/5}$ at the end of this stage, thus leading to $p \sim N^{4/5}$. Beyond this point, the growth of the “pearls” is accompanied by shortening of the bridges and the overall shrinking of the chain. The third stage, the collapse of the “pearl necklace”, involves the chain as a whole. The corresponding length scale $R_F (\sim N^{3/5})$ is larger and the characteristic time is thus longer. It is assumed that p remains roughly constant during these three stages. Eventually, the droplets come into contact, and coalesce into a single globule. Our discussion is limited to the early stages of the collapse. The last regime will not be considered in the present paper. Within this picture, the characteristic times for the first three stages, pearling, bridge-stretching and the collapse of the pearl necklace are, respectively, $\tau_p \sim N^o$, $\tau_{bs} \sim N^{1/5}$ and $\tau_{pn} \sim N^{6/5}$. The model we propose differs from the existing phenomenological descriptions in two respects. First, the two initial stages were not considered in these models. Second, the treatment of the third stage, the collapse of the pearl necklace, is different. A more detailed comparison with the phenomenological models, as well as the Langevin-type theories and to simulation studies, will be presented in the final Section.

The Paper is organized as follows. To obtain the temporal evolution of the various stages we balance the driving force with the entropy production. A discussion of this approach is presented in Section II. In Section III we recall some key results concerning collapse blobs and the thermodynamics of collapse. In addition, we discuss the initial role of the collapse blobs as spinodal “modes” and the equilibrium deformation behavior of a collapsed chain. The collapse of a chain from a good solvent to a θ solvent is discussed in Section IV. The results are then used to analyze the first stage of the collapse, i.e., the formation of nascent droplets or “pearling”. In Section V we discuss the collapse of a chain with constrained ends. This discussion is then utilized to describe the second stage of collapse, in which the stationary droplets, pearls, grow by accreting monomers from the bridges thus causing the bridges to stretch. The shrinking of the resulting string of pearls is analyzed in Section VI.

II. SOME GENERAL CONSIDERATIONS; ENTROPY PRODUCTION METHOD

The design of the phenomenological model presented in this paper, involves two steps. In the first step we propose a sequence of stages followed by the collapsing chain (The stages involved were outlined in the introduction.) The second step is to calculate the characteristic time associated with the various stages in the proposed route. A simple method for calculating the characteristic times was proposed by de Gennes [11]. It focuses on a volume element of solvent containing a single chain and coupled to a thermal reservoir that maintains a temperature T .

The systems as a whole, is closed. During collapse, the free energy of the chain F_{chain} decreases. The decrease in F_{chain} gives rise to an increase in S_{total} the total entropy of the system as a whole. Since the collapse is the only irreversible process involved the changes in F_{chain} and S_{total} are related by

$$\Delta F_{chain} = -T \Delta S_{total}. \quad (2.1)$$

The dynamics of the process are described by

$$\frac{dF_{chain}}{dt} = -T \frac{dS_{total}}{dt}. \quad (2.2)$$

To implement this argument, it is necessary to specify: (i) F_{chain} as a function of the chain radius R . One assumes that $dF_{chain}/dt = (dF_{chain}/dR)V$, where $V = dR/dt$. The form of F_{chain} for the various stages will be discussed at the appropriate sections. One must also specify (ii) the operative dissipation mechanisms that determine dS_{total}/dt in terms of R and V . This entropy production approach is independent of the model, in that its applicability is not limited to a specific choice of F_{chain} or of the dissipative modes. Nor does it provide guidance for choosing this crucial input.

Two dissipation mechanisms are considered for the various stages of collapse. First is the viscous dissipation associated with the motion of the solvent. Second is the frictional dissipation due to the Stokes drag on the chain. The magnitude of the viscous force [29] acting on a unit volume is on the order of $\eta \nabla^2 V$ where η is the shear viscosity. In the following we estimate it by $\eta V/R^2$. The associated dissipation per unit time is thus roughly $\eta V^2/R^2$ and the total hydrodynamic dissipation within a volume R^3 is $T dS_h$ as given by

$$T \frac{dS_h}{dt} \approx \eta \frac{V^2}{R^2} R^3 \approx \eta V^2 R. \quad (2.3)$$

The Stokes drag force acting on a sphere of radius r moving with a constant velocity V is $6\pi\eta Vr$, and the associated “frictional” dissipation per particle is

$$T \frac{dS}{dt} \approx \eta V^2 r. \quad (2.4)$$

To obtain the total frictional dissipation it is necessary to sum the contributions due to the hydrodynamically impenetrable objects involved in the stage considered. The number of such objects, their radius r and the relationship between r and R differ in the various stages of collapse. The de Gennes argument is equivalent to equating the frictional force to the contraction force. It allows us however, to consider on equal footing the dissipation due to Stokes drag forces and to the hydrodynamic flows. Finally, note that the dissipation increases with the length scale. This observation motivates the proposed sequence of stages which involve processes taking place at progressively larger length scales.

The familiar methods of irreversible thermodynamics [30] focus on linear responses, the Onsager relations,

and their refinements. In marked difference, the de Gennes approach is not limited to a linear regime nor does it rely on the analysis of the regression of fluctuations. The method applies to the complete dynamic range, provided that the driving forces and the dissipation mechanisms are correctly identified. The dissipative modes invoked in our discussion hold under the assumption that the hydrodynamic description is applicable to the collapse of a polymer. It is expedient to use this approach, but one should note that the validity of continuum theories at this length scale is a delicate issue.

III. COLLAPSE BLOBS, SPINODAL DECOMPOSITION AND THE EXTENSION ELASTICITY OF GLOBULES

Whilst the configurations of polymers in good and poor solvents are well understood, the nature of the transition between the two regimes is not fully resolved. Different models suggest that the transition may be continuous or discontinuous, depending on N and the stiffness of the chain. The issue of the order of the transition is, however, irrelevant when considering a collapse following a quench to the poor solvent regime. In this regime, the equilibrium configuration of the chain is determined primarily by the Flory interaction free energy F_{int} . The elasticity of the chain, i.e., its configurational entropy, plays a relatively minor role, limited to determining the structure of the globule-solvent interface [2]. In the case of a single chain, for which the translational entropy of the polymer is irrelevant, the $N \rightarrow \infty$ limit of F_{int} determines the equilibrium behavior:

$$\frac{F_{int}}{kT} = (1 - \phi) \ln(1 - \phi) + \chi \phi(1 - \phi). \quad (3.1)$$

Here, ϕ is the monomer volume-fraction and χ , the Flory parameter, is a measure of the strength of the interactions giving rise to the mixing enthalpy. For a given polymer-solvent system, χ depends only on the temperature T . In the good solvent regime, for which $\chi < 1/2$, F_{int} is a convex function of ϕ . A critical point occurs at (χ_c, ϕ_c) specified by $\chi_c = 1/2$ and $\phi_c = 0$. When $\chi > 1/2$ the solvent is poor and the plot is concave in the range $0 < \phi < \phi_+$. A common tangent construction between the origin and ϕ_+ indicates the coexistence of a dense phase, of concentration ϕ_+ and the neat solvent. The ϕ_+ phase corresponds to the collapsed globule. This amounts to setting the osmotic pressure of the polymer π within the dense phase to zero, as is expected because there are no free polymers in the solvent. The vanishing of π leads to $\ln(1 - \phi) = \phi + \chi\phi^2$. In the vicinity of the θ temperature, the $\ln(1 - \phi)$ term may be approximated by the first three terms of its Taylor expansion. The $\pi = 0$ requirement then leads to

$$\phi_+ \approx -v/2w, \quad (3.2)$$

where $v = a^3(1 - 2\chi) < 0$ is the second virial coefficient, a is the size of the monomer, and $w = 1/6 > 0$ is the third virial coefficient. Thus, ϕ_+ is determined by the balance of attractive binary monomer-monomer interactions and higher-order repulsive interactions. The chain elasticity does not play a role. In turn, ϕ_+ sets the radius of the collapsed globule via $Na^3/R^3 \approx \phi_+$, leading to $R/a \approx (N/\phi_+)^{1/3}$. The occurrence of an unstable region in $F_{int}(\phi)$ is a crucial feature of this discussion. Due to this feature, the collapse of a quenched chain exhibits certain characteristics of first-order phase transition.

The structure of the interface, and the corresponding surface tension, can not be obtained from the discussion presented above. A ‘‘blobological’’ argument can provide the missing information [4]. The configurations of a collapsed chain are characterized by a correlation length, ξ_c . On length scales smaller than ξ_c the monomer-monomer attraction is too weak to perturb the configurations of the chain, and it behaves as a random walk. This allows one to define collapse blobs, which comprise g_c monomers such that $g_c^{1/2}a \approx \xi_c$. A fully collapsed chain can be envisioned as a spherical globule composed of close-packed ξ_c -blobs. The correlation length ξ_c is determined by equating the interaction free-energy due to monomer-monomer attraction in such a chain segment to kT . The interaction free-energy is vg_c^2/ξ_c^3 , where v is the second virial coefficient. In the vicinity of the θ temperature, v may be expressed as $v \approx a^3(\Delta T/\theta)$, where $\Delta T \equiv (T - \theta)/\theta$, thus leading to

$$g_c \approx \left(\frac{\theta}{\Delta T}\right)^2, \quad \xi_c/a \approx \left(\frac{\theta}{\Delta T}\right). \quad (3.3)$$

The density ga^3/ξ_c^3 within a single blob is comparable to that of the dense phase ϕ_+ resulting from the phase separation of free polymers in a poor solvent. The ξ_c -blobs attract each other, and the unperturbed chain forms a collapsed globule of radius $R \approx (N/g_c)^{1/3}\xi_c$. A collapse blob in contact with the solvent is assigned an energy of kT . Thus, the boundary of the globule is associated with a surface free energy

$$\gamma \approx kT/\xi_c^2. \quad (3.4)$$

Note that the blob picture, as described above, is valid only when the chain comprises many collapse blobs, i.e., when the depth of the quench is such that $\theta \gg |\Delta T| \gg \theta/N^{1/2}$ and $1 \ll g_c \ll N$. We should also add that in the following we treat the ξ_c -blobs as hydrodynamically impenetrable spheres.

When N is sufficiently large, the collapsed globule may be viewed as a droplet of the dense phase with density ϕ_+ in coexistence with the neat solvent. Within our model, the first stage of collapse involves ϕ_+ droplets, pearls, that are joined by bridges which retain the configurations found in good solvent conditions. This situation is reminiscent of the condensation of a fluid droplets from a supersaturated vapor [31]. In this last situation it is

found that droplets whose radius is smaller than a critical radius r_c tend to evaporate whereas larger drops, i.e., those for which $r > r_c$, grow indefinitely. This similarity wrongly suggests that the formation of nascent pearls is analogous to the nucleation of critical droplets. This analogy is discredited by the following rough argument. The thermodynamic potential of a dense droplet coexisting with “free” monomers is given by

$$\Lambda = F(N_d) - N_d\mu, \quad (3.5)$$

where N_d is the number of monomers in the droplet, and μ is the chemical potential of the free monomers. For a sufficiently large droplet $F = N_d\mu_d + \gamma r^2$, where μ_d is the chemical potential of a monomer within the droplet. Choosing the reference state to be a blob within the droplet and assigning kT to an “uncondensed” blob, leads to

$$\frac{\Lambda}{kT} \approx -\frac{N_d}{g_c} + \left(\frac{N_d}{g_c}\right)^{2/3}, \quad (3.6)$$

which has a maximum at $N_d \approx g_c$. As Eq. (3.6) is only valid for $N_d \gg g_c$, this establishes only that there is no critical droplet of larger size. This argument does however suggest that chain segments incorporating g_c monomers play a special role in the onset of collapse. This view is consistent with the definition of a ξ_c -blob: The monomer-monomer attraction is too weak to perturb the chain configurations on smaller length scales, but is sufficient to induce collapse on length scales larger than ξ_c . It is also helpful to note that the shrinkage of a chain segment into a collapse blob does not encounter a free-energy barrier. Accordingly, a collapse blob can not be viewed as a critical droplet. Rather, the formation of a ξ_c -blob resembles spinodal decomposition with the caveat that the associated dissipation arises from configurational changes of the chain as a whole. Thus, in order to minimize the entropy production the first step of the collapse involves the formation of a small number p ($\ll N/g_c$) of collapse blobs instead of a string of N/g_c ξ_c -blobs

The concave region in F_{int} is also the origin of the force-law governing the extension a collapsed globule. When the end-to-end distance of the stretched globule is fixed, a dense globule coexists with a stretched string of ξ_c -blobs. The tension f_{co} associated with this coexistence is the driving force for the third stage of the collapse. The extension of the globule actually involves three regimes [28,32]. In the first regime the spherical form of the globule is initially deformed into a prolate ellipsoid, but maintains a constant volume corresponding to close packing of the ξ_c -blobs. Within this linear-response regime the free-energy penalty F incurred is due to the increase of the surface free energy

$$F \approx \gamma\Delta A \approx \gamma(L - R_c)^2, \quad (3.7)$$

where $\Delta A \approx (L - R_c)^2$ is the surface area increment associated with the deformation, and L is the length of

the axis of rotation. The corresponding restoring force, $f = -\partial F/\partial R$, is proportional to the strain $(L - R_c)$:

$$f \approx -\gamma(L - R_c). \quad (3.8)$$

This type of process can not proceed indefinitely. If it were pursued indefinitely, the distorted globule will assume a cylindrical shape and, eventually, form a string of ξ_c -blobs. This scenario gives rise to a van der Waals loop in the f vs. R diagram. In turn, this is indicative of instability with respect to a coexistence of a weakly elongated globule and a stretched string of ξ_c -blobs. This effect is reminiscent of the Rayleigh-Plateau instability [33] involving the break-up of a fluid jet into a succession of droplets. In the second, coexistence, regime the chain comprises a stretched string of n/g_c ξ_c -blobs and a roughly spherical globule of $(N - n)/g_c$ closely packed ξ_c -blobs. To characterize this equilibrium situation it is necessary to minimize the free energy of a stretched chain comprised of a dense globule and a string of n/g_c collapse blobs, i.e.,

$$\frac{F}{kT} \approx -\left(\frac{N - n}{g_c}\right) + \left(\frac{N - n}{g_c}\right)^{2/3} + \frac{L^2}{na^2}. \quad (3.9)$$

The first term allows for the transfer of the collapse blobs from the solvent into the “dense phase,” i.e., the interior of the globule. This is the primary driving term for the growth of the globule. The second term reflects the surface free energy of the globule. The elastic free energy of the string of blobs is described by the third term. Note that $na^2 \approx (n/g_c)\xi_c^2$ is the unperturbed span of an ideal string of collapse blobs. Making F stationary with respect to n , $\partial F/\partial n = 0$, leads to

$$\frac{1}{g_c} \left[1 - \left(\frac{N - n}{g_c}\right)^{-1/3} \right] \approx \frac{1}{g_c} \approx \frac{L^2}{n^2a^2}. \quad (3.10)$$

In the limit of large L and for $n \lesssim N$ this leads to

$$\frac{L}{\xi_c} \approx \frac{n}{g_c}. \quad (3.11)$$

The equilibrium free energy of the resulting tadpole configuration is, up to numerical prefactors

$$\frac{F}{kT} \approx \left(\frac{N - n}{g_c}\right)^{2/3} + \left(\frac{n}{g_c} - \frac{N}{g_c}\right) + \frac{n}{g_c}. \quad (3.12)$$

The first term allows for the surface free-energy γr_g^2 of a globule of radius $r_{globule} \approx [(N - n)/g_c]^{1/3}\xi_c$. The transfer free-energy of blobs into the dense phase is reflected in the second term. The third term is the stretching energy of the extended string of length $L_s \approx (n/g_c)\xi_c$ as given by the Gaussian expression for the elastic penalty kTL_s^2/na^2 . It is also possible to interpret this last term

as the surface energy of the extended string. The end-to-end distance reflects two contributions

$$L \approx \xi_c \left[\left(\frac{N-n}{g_c} \right)^{1/3} + \frac{n}{g_c} \right]. \quad (3.13)$$

The first term is the radius of the globule, and the second is the span of the stretched string of ξ_c -blobs. When n is sufficiently large we may approximate dR as $\xi_c dn/g_c$ and the corresponding force law $f = -\partial F/\partial L$ reads

$$f/kT \approx -\xi_c^{-1} + r_{globule}^{-1}. \quad (3.14)$$

It is important to note that f decreases as $r_{globule}$ approaches ξ_c . This finite-size correction is reminiscent of the Laplace law for the vapor pressure of small droplets. It is negligible over a wide range of extensions if N is large enough. Because of this correction different deformation scenarios are expected for the $f = const'$ and the $L = const'$ ensembles. In the first case the globule unravels completely as soon as a critical force $f_{co}/kT \approx 1/\xi_c$ is applied. No globule-coil coexistence is expected. Such a coexistence is however expected when an end-to-end distance is imposed. In this case the tension in the string is f_{co} . The onset of the coexistence occurs when $L \approx R_c + \xi_c$ as can be seen by equating f_{co}/kT to the force given by Eq. (3.8). The upper boundary of this second regime corresponds to a fully extended string of blobs, $L_{max} \approx (N/g_c)\xi_c$. Stronger extension is characterized by simple Gaussian elasticity, up to the onset of finite extensibility effects.

IV. COLLAPSE TO θ CONDITIONS AND THE FORMATION OF NASCENT DROPLETS

A quench from $T > \theta$ to $T = \theta$ causes the chain to shrink from $R_F/a \approx v^{1/5}N^{3/5}$ to $R_o/a \approx N^{1/2}$ (Fig. 2). The dynamics of this process are of interest for two reasons. First, as we shall discuss, the formation of nascent pearls follows similar kinetics. Second, the discussion of this process is especially simple, thus providing a useful introduction to the subsequent sections. The quench to $T = \theta$ turns off the repulsive interactions between the monomers so that driving force for the ‘‘collapse to θ ’’ is due solely to the Gaussian elastic free energy of the chain, $F_{chain} \approx F_{el}$ or

$$\frac{F_{el}}{kT} \approx \alpha^2 - \ln \alpha, \quad (4.1)$$

where $\alpha = R/R_o$ and $R = R(t)$ is the instantaneous chain radius at time t . To obtain the characteristic time for this process we equate the time derivative of the elastic energy,

$$\frac{dF_{el}}{dt} \approx \left(\alpha - \frac{1}{\alpha} \right) \frac{d\alpha}{dt}, \quad (4.2)$$

to the dissipative losses associated with the shrinking, $-TdS_{total}/dt$, where dS_{total}/dt is the corresponding entropy production. Two dissipation processes are involved. One is the viscous dissipation due to the hydrodynamic flow resulting from the contraction of the coil. As was discussed previously, the resulting entropy production within the coil is roughly

$$T \frac{dS_h}{dt} \approx \eta V^2 R, \quad (4.3)$$

where $V = dR/dt$ is the velocity of the flow. Second is the entropy production due to the Stokes drag force experienced by the monomers as they move through the solvent. The associated entropy production is approximately

$$T \frac{dS_s}{dt} \approx \eta N a V^2. \quad (4.4)$$

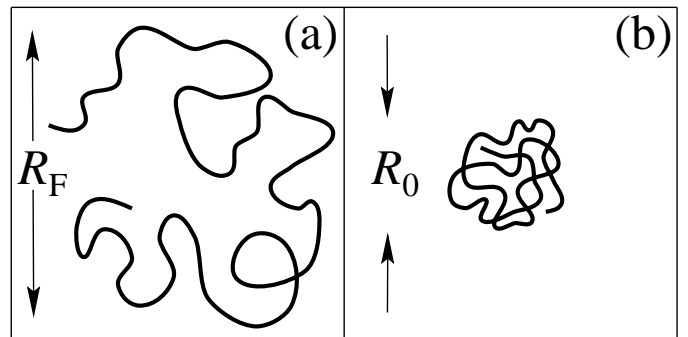


FIG. 2. Collapse to θ conditions: (a) initial, self-avoiding configuration; (b) the final, random walk configuration.

The dynamics of the collapse are determined by $dF_{el}/dt = -T(dS_h/dt + dS_s/dt)$. Whilst in this case it is possible to solve the full equation, it is easier, and more instructive, to consider $dF_{el}/dt = -TdS_h/dt$ and $dF_{el}/dt = -TdS_s/dt$ separately. $dF_{el}/dt = -TdS_h/dt$ leads to

$$\frac{dt}{\tau_Z} \approx \frac{\alpha^2 d\alpha}{\alpha^2 - 1}, \quad (4.5)$$

and the characteristic time associated with the hydrodynamic dissipation is thus the Zimm time [1] of the ideal coil, i.e.,

$$\tau_Z \approx \frac{\eta R_o^3}{kT} \sim N^{3/2}. \quad (4.6)$$

The frictional dissipation is dominant as it scales with N rather than R . It leads to

$$\frac{dt}{N^{1/2}\tau_Z} \approx \frac{\alpha d\alpha}{\alpha^2 - 1}, \quad (4.7)$$

and the corresponding characteristic time is the Rouse relaxation time [1] of an ideal coil $\tau_R \approx \eta N^2 a^3 / kT$ or

$$\tau_R \approx \tau_Z N^{1/2} \sim N^2. \quad (4.8)$$

As the Rouse time is much longer, it dominates the process.

Within our picture, the first stage of the collapse is the formation of nascent pearls comprising each of roughly g_c monomers. The process involves p randomly distributed chain segments. Initially, each of the chain segments exhibits self-avoidance. Once the solvent is quenched, the monomer-monomer repulsions disappear and the segments shrink to their ideal coil configuration. As the nascent pearls consist of only g_c monomers the monomer-monomer attraction is not strong enough to perturb the ideal coil configuration within them. So long as p is small enough, the overall radius of the chain is only weakly modified and the dissipation is due to the local configurational changes. In this picture it is possible to neglect the couplings between the droplets and between the droplets and the chain as whole. Thus, the dynamics of this process are essentially identical to those of the collapse of a chain comprising g_c monomers to θ conditions. The characteristic time is, accordingly the corresponding Rouse time or

$$\tau_p \approx \tau_\xi g_c^{1/2} \approx \frac{\eta a^3}{kT} g_c^2 \sim \left(\frac{\theta}{\Delta T} \right)^4, \quad (4.9)$$

where

$$\tau_\xi \approx \frac{\eta \xi_c^3}{kT} \sim \left(\frac{\theta}{\Delta T} \right)^3, \quad (4.10)$$

is the Zimm time of a collapse blob. Note that τ_p is independent of N and p as expected for a local process. A short relaxation time scaling as N^0 is also predicted by Langevin type theories of collapse [8,10].

V. COLLAPSE OF A CHAIN WITH CONSTRAINED ENDS: THE BRIDGE-STRETCHING REGIME

In the second stage of the collapse, the roughly stationary droplets, “pearls”, grow by “sucking in” monomers from the bridges joining them. This stage ends when the initially undeformed bridges assume the configuration of a stretched string of ξ_c -blobs. In comparison to the “spinodal” stage described in Section IV, this process is distinguished by two features. First, the driving force is now due to the transfer free energy of the free monomers into the dense phase. Second, the evolution of the droplets at this stage strongly affects the configuration of the bridges. The bridges stretch as the number of monomers in them decreases. We first consider the somewhat simpler situation of the collapse of a chain with its

ends constrained to fixed positions separated by a distance $L \gg R_c$ (Fig. 3). The free energy of such a chain, neglecting the surface free-energy, is given by

$$\frac{F_{chain}}{kT} \approx - \left(\frac{N-n}{g_c} \right) + \frac{L^2}{na^2}, \quad (5.1)$$

where n is the number of “free” monomers that have not been assimilated into a globule. We assume that the n monomers behave as a random walk, i.e., the instantaneous span of the chain perpendicular to the end-to-end vector is

$$R_\perp \approx (n/g_c)^{1/2} \xi_c \approx n^{1/2} a, \quad (5.2)$$

and as a result

$$\frac{dn}{dt} \approx \frac{1}{a^2} R_\perp \frac{dR_\perp}{dt}. \quad (5.3)$$

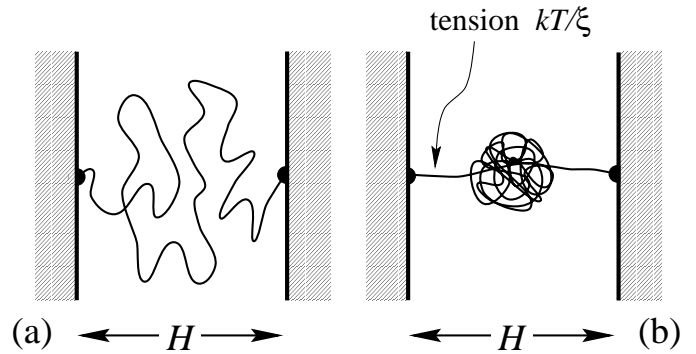


FIG. 3. Collapse of chain with constrained ends: (a) the initial, swollen configuration; (b) the final “tadpole” configuration in a poor solvent.

Relations (5.2) and (5.3) are actually invalid at the initial stages of this regime, when the configurations of the chain still exhibit self-avoidance. They are, however, expected to apply at the final stages, which dominate the relaxation time. Invoking them implies that the relaxation of the chain configuration when n decreases is effectively instantaneous. The driving force for this stage, as specified by Eqs. (5.1)-(5.3), is

$$\frac{1}{kT} \frac{dF_{chain}}{dt} \approx \left(\frac{1}{g_c} - \frac{L^2}{n^2 a^2} \right) \frac{1}{a^2} R_\perp \frac{dR_\perp}{dt}. \quad (5.4)$$

The driving force is opposed by the two dissipation mechanism invoked in Section IV. In the present situation, however, the dissipation reflects the cylindrical symmetry of the system. The hydrodynamic dissipation, due to the flow of the solvent as it is expelled from the region occupied by the coil, is $T(dS_h/dt) \approx \eta(dR_\perp/dt)^2 L$. The Stokes drag on the bridges formed by the collapsed blobs is $T(dS_b/dt) \approx \eta(n/g_c)\xi_c(dR_\perp/dt)^2$. The dynamics of the collapse are determined by $dF_{chain}/dt = -T(dS_{total}/dt)$. At equilibrium, n is $n_{eq} \approx (L/\xi_c)g_c \approx g_c^{1/2}(L/a)$. Introducing the variable $y = n/n_{eq}$ we obtain

$$\frac{\xi_c}{L} \frac{dt}{\tau_\xi} \approx -\frac{y dy}{y-1}, \quad (5.5)$$

and the characteristic time for this collapse process is thus

$$\tau \approx \frac{L}{\xi_c} \tau_\xi. \quad (5.6)$$

A similar scenario occurs in the bridge-stretching regime (Fig. 1). In this stage the p randomly placed pearls are roughly stationary, and they grow by assimilating monomers from the bridges joining them. The bridges are initially undeformed. This stage ends when the bridges consist of a stretched string of collapse blobs. The average length of each stretched bridge is $R_p \approx (n/g_c p) \xi_c$. As, within this model, the p bridges are randomly placed, the overall span of the chain is $R \approx p^{1/2} R_p$. By assuming that at this stage the overall size of the chain remains $R \approx R_F \approx N^{3/5} a$ and that $n \approx N$ we are led to the result

$$p \approx N^{4/5} / g_c. \quad (5.7)$$

This amounts to the completion of all short length-scale process prior to the onset of the overall shrinking of the chain. The growth of the dissipation with the length-scale involved justifies this estimate. Clearly, this is a rough estimate and, in reality, R is expected to shrink somewhat. The estimated value of p , Eq. (5.7), specifies R_p at the end of the stretching stage to be

$$R_p \approx N^{1/5} \xi_c \quad (5.8)$$

and the corresponding characteristic time is than

$$\tau_{bs} \approx N^{1/5} \tau_\xi \quad (5.9)$$

In contrast with τ_p , the time scale τ_{bs} , depends on both p and N .

VI. COLLAPSE OF THE ‘‘PEARL NECKLACE’’

At the end of the bridge-stretching regime, the configuration of the chain is that of a random walk of p steps of length R_p and with an overall radius $R_F \sim N^{3/5}$. The $p \approx N^{4/5} / g_c$ elementary steps are dumb-bells comprising of two pearls joined by a stretched string of ξ_c -blobs. It is impossible to incorporate more monomers into the pearls while keeping them stationary. The pearls can only grow by shortening the bridges, thus causing the overall shrinking of the chain from $R \sim R_F$ to $R \approx R_c \sim N^{1/3}$. It is assumed that the pearls are the vertices of a random walk and that their number, p , is constant. This approximation is reasonable in the early phase of this stage but may be questionable at later times. This issue will be discussed later. On short time-scales the bridges equilibrate rapidly whereas the pearls remain essentially fixed

in space. Consequently, the positioning of the pearls does not give rise to an entropy and the free energy corresponding to this process is $F \approx p F_{pb}$, where F_{pb} is the free energy of a pearl attached to a stretched string of collapse blobs. In turn, F_{pb} comprises two terms. One is the excess free energy of a ‘‘free’’ collapse blob as given by the kT per blob Ansatz. The second is the elastic free energy of the stretched bridge of length R_p with respect to its reference state, i.e., a random walk of collapse blobs. The span of an undeformed bridge with an ideal coil configuration is $R_{p0} \approx (n/pg_c)^{1/2} \xi_c$ and the associated Gaussian stretching penalty is $kT(R_p/R_{p0})^2$. Assuming that the overall configuration is that of a random walk, $R \approx p^{1/2} R_p$, the free energy of the chain as a whole is given by

$$\frac{F_{chain}}{kT} \approx p \left(-\frac{N-n}{pg_c} + \frac{R^2}{na^2} \right). \quad (6.1)$$

The equilibrium state of the chain, at a given instant, is specified by $\partial F / \partial n = 0$ for constant R and p , thus leading to

$$R \approx \frac{na}{\sqrt{pg_c}}. \quad (6.2)$$

We assumed that the decrease in R is slow in comparison to the relaxation of n for a given R . Accordingly, the free energy for a certain R , as obtained from Eqs. (6.1) and (6.2) is given by

$$\frac{F_{chain}}{kT} \approx -\frac{N}{g_c} + \sqrt{p} \frac{R}{\xi_c}, \quad (6.3)$$

and the corresponding force, $f/kT \approx \partial F / \partial R$, is

$$f \approx \sqrt{p} \frac{kT}{\xi_c} \approx \sqrt{p} f_{co}, \quad (6.4)$$

where $f_{co} \approx kT/\xi_c$ is the equilibrium tension in the dumb-bell shaped, coexistence configuration. If the string of pearls is perfectly collinear, $R \approx p R_p$, similar considerations lead to $R \approx (n/g_c) \xi_c$ and $f \approx f_{co}$. In this situation only the terminal pearls experience a net force. As the tension in the bridges, ignoring finite size effects, is f_{co} , the net force on the middle pearls is zero. However, if the pearls are the vertices of a random walk, each pearl is subject to a random force $\sim f_{co}$ thus leading to (6.4). The thermodynamic driving force for the collapse is simply $dF_{chain}/dt \approx f dR/dt$. This reflects the rate of change in the number of ‘‘free’’ ξ_c -blobs, $d(n/g_c)/dt$. As before, two dissipation mechanisms are involved. The hydrodynamic dissipation is $T(dS_h/dt) \approx \eta(dR/dt)^2 R$. The dissipation modes in pearl necklace situation differs from the stretched-bridges case in two respects. First, $R(t)$ replaces $L \approx const'$ because the coil is assumed to shrink as a sphere. Second, as the pearls are no longer stationary it is necessary to consider two dissipation modes associated with the Stokes drag force. One is due, as before, to the contribution of the stretched

bridges whereas the second arises from the motion of the hydrodynamically impenetrable pearls. The pearls term is $T(dS_p/dt) \approx p\eta r_p (dR/dt)^2$, where the volume of a pearl of closed packed ξ_c -blobs, $r_p^3 \approx (N-n)/pg_c$, specifies the radius of an individual pearl. The bridges term is, similarly, $T(dS_b/dt) \approx p\eta R_p (dR/dt)^2$, where $R_p \approx (n/g_c)\xi_c$ is the length of an individual bridge. Altogether, $dF_{chain}/dt = -T(dS_{total}/dt)$ leads to

$$pg_c \frac{dt}{\tau_\xi} \approx - \left[\frac{n}{\sqrt{pg_c}} + p \left(\frac{N-n}{pg_c} \right)^{1/3} + \frac{n}{g_c} \right] dn, \quad (6.5)$$

where the three terms on the right hand side correspond, respectively, to the dissipation due to hydrodynamic flow, the pearls and the bridges. In this case it is simpler to solve individually each $dF_{chain}/dt = -T(dS_i/dt)$, in order to find the characteristic time for the different dissipation modes and then to identify the dominant one. The hydrodynamic dissipation yields

$$\tau_h \approx \left(\frac{N}{g_c} \right)^2 p^{-3/2} \tau_\xi, \quad (6.6)$$

whereas the bridges contribution leads to

$$\tau_b \approx \left(\frac{N}{g_c} \right) p^{-1} \tau_\xi, \quad (6.7)$$

and the pearls dissipation to

$$\tau_{pd} \approx \left(\frac{N}{g_c} \right)^{4/3} p^{-1/3} \tau_\xi. \quad (6.8)$$

Estimating p by $p \approx N^{4/5}/g_c$ yields $\tau_h \sim N^{4/5}/g_c^{1/2}$, $\tau_b \sim N^{6/5}/g_c$, and $\tau_{pd} \sim N^{16/15}/g_c$ leading to the identification of $\tau_b \approx (N^{6/5}/g_c)\tau_\xi$ as the longest relaxation time and the bridges dissipation as the rate-determining dissipation mode. Note, however, that this is the case only for sufficiently deep quenches, when $g_c < N^{2/5}$. By contrast, hydrodynamic dissipation is dominant when $g_c > N^{2/5}$.

The discussion presented above is based on three assumptions: (i) Finite-size corrections are negligible and $f_{co} \approx kT/\xi_c$. (ii) The pearls are placed at the vertices of a random walk (iii) $p \gg 1$ and $p \approx const'$. The first assumption is easiest to justify. The finite size correction to f_{co} is $1/r_p$, where r_p is the radius of the pearl. This correction is expected to be small at the end of the bridge-stretching stage. In any case, it decreases with time. The second assumption is reasonable, within our model, at the onset of the collapse of the pearl necklace. Its range of validity is however uncertain. Some simulation results support this picture [15] whilst others [17] suggest that the chain may approach a linear configuration. The assumption that $p \gg 1$ is reasonable for $N \gg 1$. Both [15] and [17] support this view. The assumption of $p \approx const'$ is clearly a rough approximation and p is

expected to decrease with time. It is nevertheless interesting to note that both [15] and [17] suggest that p varies very weakly over a wide range of times. ‘‘Pearl-pearl’’ coalescence is the most likely mechanism for the decrease in p . Initially, this is due to one-dimensional diffusion of the pearls that coalesce upon contact because of the surface free energy. At this point it is useful to consider two possible scenarios for the coalescence of the pearls. In the first, pearl diffusion is fast in comparison to the overall collapse of the chain. In this case the one dimensional diffusion incurs no free-energy penalties as long as n is constant. The favored mode thus involves the transfer of monomers between two adjacent bridges and through the adjoining pearl. This transfer of monomers across the pearl must take place along the trajectory of the chain. It is, thus, a reptation type motion in the sense that the monomer needs to diffuse across a distance $(r_p/a)^3 a$ instead of r_p . This dissipation mode may well dominate over the Stokes drag force. Only the terminal pearls may diffuse in a non-reptative mode. In the other limit the pearl diffusion is relatively fast. In this case it can result from asymmetry in the rate of assimilating monomers from the two bridges. In this situation, the diffusion coefficient will reflect the Stokes drag force on the pearls. In any case, the dynamics of diffusion-controlled coalescence in one-dimensional is complex. The case of the $A + A \rightarrow A$ reaction, with constant diffusion coefficient D , was studied extensively [34], and a rigorous solution was reported only recently [35]. At short times the linear concentration, c , follows the mean-field rate equation $dc/dt \propto -c^2$. However, the asymptotic solution at large times is $c \sim 1/\sqrt{Dt}$ instead of $c \sim 1/Dt$, as predicted by the mean-field treatment. The situation encountered in the present case is more complicated in two respects: First, the diffusion coefficient is no longer a constant. Rather, it depends on r_p and thus on t . Second, the total length varies with p and r_p thus introducing a novel mechanism for the t dependence of c . A complete analysis of this problem is beyond the scope of the present paper. It is however possible to estimate a characteristic time, τ_{pp} , for the onset of coalescence. τ_{pp} may be identified with the time required by a pearl in order to diffuse across a distance $R_p \approx N^{1/5}\xi_c$, as specified by the Einstein diffusion relation $D_p\tau_{pp} \approx R_p^2$. A lower bound for τ_{pp} is obtained by assuming that the diffusion coefficient of the pearl scales as $D_p \sim 1/\xi_c$ thus leading to $\tau_{pp} \sim N^{2/5}$.

VII. CONCLUDING REMARKS

The literature concerning the theory of the dynamics of collapse describes three different approaches: Langevin-type theories, simulation studies and phenomenological models. It is simplest to compare the present model to the earlier phenomenological models. The kinetics of collapse were first considered by de Gennes in 1985 [11]. In

this model the collapsing chain was viewed as a “sausage” of collapse blobs. With time, the sausage diameter increases and its length decreases. The driving free energy was identified with the interfacial free energy and the dissipation was attributed to hydrodynamic flow. A different view was later proposed by Buguin, Brochard-Wyart and de Gennes [12]. Within this model the driving free energy is the transfer free energy into the dense phase. Two scenarios were considered for the early collapse. In one, the pearls form the vertices of a random walk. This scenario differs from the present model in two respects. First, the bridges joining the pearls are assumed to be unstretched. Second, the associated dissipation arises only from the hydrodynamic flow. Importantly, the collapse time within this picture does not depend on the number of pearls, p . In the second scenario, the chain is envisioned as a dumb-bell consisting of two pearls, $p = 2$, joined by a stretched string of collapse blobs. The dissipation in this case is attributed to the Stokes drag force on the pearls. Most recently the problem was re-examined by Klushin [13]. In this model the driving free energy is the transfer free energy to the dense phase and the dissipation is due to the Stokes drag force. The chain is envisioned as a self-avoiding random walk of Kuhn lengths. In turn, these can comprise either stretched bridges joining pearls or by a sequence of collinear pearls connected by stretched bridges. Thus, the number of Kuhn lengths can change either because of coalescence or because of the formation of a collinear sequence. The rate of change in the number of Kuhn lengths is assumed to follow unimolecular kinetics. The characteristic time for this process is identified with that of a shrinking dumb-bell, assuming a constant size of the pearls. The number of pearls within a collinear sequence is assumed to decrease because monomer transfer or coalescence, both driven by the surface free-energy. Within this model, the collapse is largely due to the decrease in p . The models of Buguin et al. and of Klushin focus, in effect, on the kinetics of the collapse of a pearl necklace and do not consider possible earlier events.

In principle, the Langevin equation can provide a complete description of the collapse on all time-scales and thus allows for a systematic analysis of the problem. Unfortunately, a rigorous and complete solution of the appropriate Langevin equation is difficult. Accordingly, all the Langevin-type theories introduce certain approximations so as to reach a mathematically tractable formalism. The treatment is mathematically demanding, and often requires numerical calculations. A detailed comparison with phenomenological theories is difficult because of the very different formulations. It is interesting however to note that both the theory of Garel *et al.* [10] and of Kuznetsov et al. [8] distinguish between two regimes in the early collapse: first, a very fast process, whose characteristic time is independent of N and is thus interpreted as local rearrangement; and second, a much slower process, reflecting large scale reorganization, with a characteristic time that increases with N .

We hope that a full picture of the kinetics of collapse will eventually emerge from molecular dynamics simulations involving a polymer chain as well as solvent molecules. The currently available simulation studies do not account fully for hydrodynamics thus introducing an uncertainty in the interpretation of the results. In certain studies the interpretation is further hampered by the imposition of an “all trans” initial state [14,16]. With this caveat, the simulations mostly support the notion that the collapse involves a string of pearls joined by stretched bridges as an intermediate stage. The configuration adopted by the string of pearls is less clear. Snapshots of the chain configuration as obtained by Langevin-equation simulation of Byrne et al. [15] suggest an almost collinear string of pearls. The visualization of configurations obtained by Monte Carlo simulation of Kuznetsov et al. [17] reveal a random walk pearl necklace. These last two studies also suggest that the first step of the collapse involves the formation of localized clusters, and that subsequent cluster growth is attained by assimilating monomers from the bridges thus causing stretching. *Acknowledgments:* The authors have benefited from extensive discussions with A. Yu. Grosberg. Support from NSF-INT96-03228 (A.H., P.M.G.), CNRS-NSF US-France Cooperative Research Grant (A.H.), and NSF-DMR99-75187 (P.M.G.) is gratefully acknowledged.

-
- [1] P. G de Gennes *Scaling Concepts in Polymer Physics*, Cornell University Press, Ithaca, N.Y. (1979).
 - [2] A. Yu. Grosberg and A. R. Khokhlov, *Statistical Physics of Macromolecules*, AIP Press, New York (1994).
 - [3] J. des Cloizeaux and G. Jannink, *Polymers in Solution* Clarendon Press, Oxford (1990).
 - [4] C. Williams, F. Brochard and H.L. Frisch, *Annu. Rev. Phys. Chem.* 32, 433 (1981).
 - [5] B. Chu, Q. Ying, A. Yu. Grosberg, *Macromolecules*, 28, 180 (1995).
 - [6] C. Wu and S. Zhou, *Phys. Rev. Lett.* 77, 3053 (1996).
 - [7] M. Nakata and T. Nakagawa, *Phys. Rev. E* 56, 3338 (1997).
 - [8] (a) E.G. Timoshenko and K.A. Dawson, *Phys. Rev E* 51, 492 (1995); (b) E.G. Timoshenko, Yu. A. Kuznetsov and K.A. Dawson, *J. Chem. Phys.* 102, 1816 (1995); (c) Yu. A. Kuznetsov, E.G. Timoshenko and K.A. Dawson, *J. Chem. Phys.* 104, 3338 (1996).
 - [9] F. Ganazzoli, R. La Ferla and G. Allegra, *Macromolecules*, 28, 5285 (1995).
 - [10] T. Garel, H. Orland and E. Pittard, in *Spin Glasses and Random Fields*, edited by A. P. Young (World Scientific, Singapore, 1998).
 - [11] P.G. de Gennes, *J. Phys. (Paris) Lett.* 46, L-639 (1985).
 - [12] A. Buguin, F. Brochard-Wyart, P. G. de Gennes, *C. R. Acad. Sci. Paris* 322 IIB, 741 (1996).
 - [13] L. L. Klushin, *J. Chem. Phys.* 108, 7917 (1998).

- [14] T. A. Kavassalis and P.R. Sundararajan, *Macromolecules* 26, 4144 (1993).
- [15] A. Byme, P. Kieman, D. Green and K.A. Dawson, *J. Chem. Phys.* 102, 573 (1995).
- [16] G. Tanaka and W. L. Mattice, *Macromolecules*, 28, 1049 (1995).
- [17] Yu. A. Kuznetsov, E.G. Timoshenko and K.A. Dawson, *J. Chem. Phys.* 103, 4807 (1995).
- [18] M. Wittkop, S. Kreitmeier and D. Göritz, *J. Chem. Phys.* 104, 3373 (1995).
- [19] B. Ostrovsky and Y. Bar-Yam, *Europhys. Lett.* 25, 409 (1994).
- [20] A. Milchev and K. Binder, *Europhys. Lett.* 26, 671 (1994).
- [21] A. Yu. Grosberg, S.K. Nechaev and E.I. Shakhovich, *J. Phys. (Paris)* 49, 2095 (1988).
- [22] Y. Rabin, A. Yu. Grosberg and T. Tanaka, *Europhys. Lett.* 32, 505 (1995).
- [23] A. Yu. Grosberg and D. Kuznetsov, *Macromolecules*, 26, 4249 (1993).
- [24] G. Raos and G. Allegra, *Macromolecules*, 29 8565 (1996), and 29, 6663 (1996); *J. Chem. Phys.* 104, 1626 (1996).
- [25] T. E. Creighton, Ed. *Protein Folding*, Freeman, New York (1994).
- [26] V. S. Pande, A. Yu. Grosberg, T. Tanaka and D. S. Rokhsar, *Curr. Opin. Struct. Biol.* 8, 68 (1998).
- [27] E.I. Shakhovich, *Curr. Opin. Struct. Biol.* 7, 29 (1997).
- [28] A. Halperin and E.B. Zhulina, *Europhys. Lett.* 15, 417 (1991); *Macromolecules* 24, 5393 (1991).
- [29] D.J. Acheson, *Elementary Fluid Dynamics*, Clarendon Press, Oxford (1990).
- [30] H. B. Callen, *Thermodynamics and an Introduction to Thermostatistics*, John Wiley (1985).
- [31] S. K. Ma, *Statistical Mechanics*, World Scientific, Singapore (1985).
- [32] Simulation studies of extended chains in poor solvents support the picture presented in Ref. [28]. P. Cifra and T. Bleha, *Macromol. Theory Simul.* 4, 233 (1995); and *J. Chem Soc. Faraday Trans.* 91, 2465 (1995); S. Kreitmeier, M. Wittkop and D. Göritz, *J. Comp. Phys.* 112, 267 (1994); M. Wittkop, S. Kreitmeier, and D. Göritz, *Phys. Rev. E* 53, 838 (1996); and *J. Chem Soc. Faraday Trans.* 92, 1375 (1996).
- [33] T. E. Faber, *Fluid Dynamics for Physicists*, Cambridge University Press (1995).
- [34] V. Privman, C.R. Doering and H.L. Frisch, *Phys. Rev. E* 48, 846 (1993).
- [35] D. ben-Avraham, *Phys. Rev. Lett.* 81, 4756 (1998).